ASTM INTERNATIONAL

Journal of Testing and Evaluation

Yuzhu Liu,[1] Ying Chen,[2] Wei Zeng,[3] Dongyun Luo,[1] Pan Hu,[4] Xuming Huang,[1] and Shangzhi Yu[1]

DOI: 10.1520/JTE20220356

A Method of Quantitative Detection of Fatigue Crack Depth in Bottom Rails by Ultrasonic Guided Waves Based on PCA-SVM

Journal of Testing and Evaluation

doi:10.1520/JTE20220356 available online at www.astm.org

Yuzhu Liu,[1] Ying Chen,[2] Wei Zeng,[3] Dongyun Luo,[1] Pan Hu,[4] Xuming Huang,[1] and Shangzhi Yu[1]

A Method of Quantitative Detection of Fatigue Crack Depth in Bottom Rails by Ultrasonic Guided Waves Based on PCA-SVM

Reference

Y. Liu, Y. Chen, W. Zeng, D. Luo, P. Hu, X. Huang, and S. Yu, "A Method of Quantitative Detection of Fatigue Crack Depth in Bottom Rails by Ultrasonic Guided Waves Based on PCA-SVM," *Journal of Testing and Evaluation* https://doi.org/10.1520/JTE20220356

Manuscript received July 8, 2022; accepted for publication October 21, 2022; published online February 8, 2023.

[1] School of Electronic and Information Engineering, Jiujiang University, No. 551 Qianjin Rd., Lianxi District, Jiujiang City, Jiangxi Province 332005, China

[2] School of Literature, Jiujiang University, No. 551 Qianjin Rd., Lianxi District, Jiujiang City, Jiangxi Province 332005, China

[3] School of Electronic and Information Engineering, Jiujiang University, Lianxi District, Jiujiang City, Jiangxi Province 332005, China (Corresponding author), e-mail: 270401671@qq.com, https://orcid.org/0000-0002-2821-7792

[4] School of Electrical Engineering, Nantong University, No. 9 Siyuan Rd., Chongchuan District, Nantong City, Jiangsu Province 226019, China

ABSTRACT

Ultrasonic guided wave is widely used to detect cracks in rail because of its long propagation distance and small attenuation. To effectively detect the fatigue crack in rail bottom through ultrasonic guided wave, an improved principal component analysis-support vector machine (PCA-SVM) intelligent algorithm based on grid search (GS) is proposed to detect the fatigue crack at different depths of rail bottom. The finite element method is used to establish the model of ultrasonic guided wave at different depths of the rail bottom, and the simulation model is compared with the experimental data to determine the effectiveness of the simulation model. Five main component features of the fatigue cracks at different depths are extracted by PCA. The GS method is used to optimize the penalty factor *c* and kernel function parameter *g* in the SVM, and the optimized SVM model is selected to identify the rail fatigue crack at different depths. The combination of theoretical simulation and experimental results shows that the accuracy of the training set and the test set of the improved PCA-SVM intelligent algorithm based on the GS method can reach 99.79 % and 99.73 %, respectively, which provides a basis and method for the detection of the fatigue crack depth of the rail bottom.

Keywords

ultrasonic guided wave, support vector machine, fatigue cracks

Introduction

In the high-speed railway system, because the rail is an important piece of equipment for supporting the train load and guiding the train wheels, it will inevitably produce various fatigue cracks during heavy train operation such as rail deformation, fatigue cracks, and even fracture. These rail fatigue cracks directly threaten driving safety and are the biggest hidden dangers in the transportation process. The rail fatigue cracks mainly include surface fatigue cracks, stress corrosion, peeling, and subsurface or internal cracks. Among them, the fatigue cracks at the switch rail, welding joint, rail waist, and rail bottom cannot be effectively detected, which puts forward higher requirements for on-line nondestructive testing of the railway rails. Ultrasonic guided wave is widely used in rail crack detection because of its long propagation distance and small attenuation.[1–8]

When the ultrasonic guided wave propagates in the rail, because of the special shape and complex structure of the rail, the ultrasonic guided wave will produce a dispersion phenomenon and mode conversion. Therefore, the ultrasonic guided wave signals in different modes that can be distinguished after a series of signal processing.[9–12] Taweel, Dong, and Kazic proposed using the semi-analytical finite element method (SAEM) to calculate the propagation characteristics of the guided waves in various regular or irregular structures, and this method has become one of the ways to study the characteristics of the guided waves.[13] Coccia et al. used this method to analyze the propagation characteristics of the guided waves at the railhead.[14] Hayashi et al. developed a rail dispersion software using this method to obtain the dispersion curve of the ultrasonic guided wave propagation in the rail.[15] In addition to the SAEM, Sanderson and Smith calculated the dispersion curve of a 0–60 kHz low-frequency ultrasound guided wave in the rail by using the specific frequency analytic method.[16] Palmer et al. used a 200-kHz low-frequency broadband surface wave excited by the electromagnetic acoustic transducer to detect the rail cracks and obtain the relationship between the rail crack depth and cutoff frequency.[17]The researchers extracted the features of the corrosion defects on the rail bottom, including the maximum amplitude, peak power frequency, median power frequency, and short-time Fourier transform coefficient, and realized the classification and recognition of the corrosion defects on the rail using support vector machine (SVM).[18] Cunfu et al. calculated the dispersion curve of the guided wave in the rail by the characteristic frequency method and effectively analyzed the guided wave mode and frequency suitable for the rail inspection. Because the ultrasonic guided wave excited in the rail will produce a dispersion phenomenon and mode conversion, to obtain a single-mode signal, the signal must be processed to distinguish the guided wave signals in different modes.[19] The common signal analysis method includes/involves the time domain, the frequency domain, the time-frequency domain, and other signal processing methods.[20,21] In this paper, the machine learning algorithm is combined with the fatigue crack identification method to quantitatively evaluate the fatigue cracks in the rail bottom.[22] Compared with the machine learning methods, such as the artificial neural networks and the decision trees, SVM can effectively avoid problems such as over-fitting, under-fitting, and local extreme values in the algorithm calculation process.[23,24]

In this paper, an intelligent algorithm based on principal component analysis (PCA)-SVM is proposed to detect the fatigue crack depth of the rail bottom. The data samples are obtained through the theoretical simulation and experiment, and then five main component features of the fatigue cracks at different depths are extracted by the PCA method. The SVM model is optimized by the grid search (GS) method to identify the fatigue crack depth of the rail bottom. This study is mainly divided into four parts. The second part introduces the finite element (FE) model of the ultrasonic guided wave in the rail bottom, the experimental method, and the PCA algorithm and the related principle of SVM. The third part mainly analyzes the performance of the ultrasonic guided wave of the PCA-SVM model in detecting the fatigue crack depth of the rail bottom. The PCA-SVM model proposed in this paper has a good detection effect on the fatigue crack depth of the rail bottom. The fourth part gives the conclusion.

Experimental Method and Processing Method

EXPERIMENTAL SETUP

The experimental system is shown in figure 1. In the experimental process, a 60-kg/m rail with a length of 1 m is selected as the experimental object. The piezoelectric ceramic chip is PZT-5 with a diameter of 10 mm, a thickness of 1 mm, and a center frequency of 200 kHz. The arbitrary function generator is Tektronix AFG31000, the preamplifier is CTS-8682d, the magnification is 30 dB, the bandwidth is 20 kHz–20 MHz, the power amplifier is KM7602m, the analog signal/digital signal (A/D) is USB8504, and the host computer software platform is matlab2021.

The sampling frequency of the A/D is 5 MHz, the total number of sampling points is 1,001, and the total sampling time is 200 μs. During the experiment, to reduce random ambient noise, the ultrasonic wave needed to be averaged 50 times. The distance between the transmitting sensor and the receiving sensor is 10 cm, and the fatigue crack is located at the center of the sensor. The fatigue crack of the rail bottom was selected for the experiment. The fatigue crack depths are 2 mm, 4 mm, 6 mm, 8 mm, 10 mm, and 12 mm, and the width is 0.5 mm. Six kinds of fatigue crack run through the rail bottom. In the experiment, the signal used to excite the piezoelectric ceramic sheet is the center frequency of 200 kHz, and an arbitrary function generator is used to generate a five-cycle sinusoidal signal modulated by Hanning, as shown in figure 2. During the simulation process, to further increase the regression model data sample, the Abaqus software was used for the ultrasonic guided wave simulation. In the FE simulation, the fatigue crack depths are 2 mm, 2.5 mm, 3 mm, 3.5 mm, 4 mm … 12 mm, and the width is 0.5 mm. Twenty-one kinds of the fatigue crack run through the rail bottom.

NUMERICAL MODEL AND SIMULATION

The rail bottoms studied in this paper are the 60-type steel rail laid on the high-speed railway in China. The standard section size of the 60-type rail is based on the size of the actual high-speed rail. A three-dimensional (3D) model is established using Pro/E software, as shown in figure 3*A*. The length of the 3D rail model is 1 m. The material characteristics of the 60-type rail are shown in Table 1. The FE simulation software Abaqus is used to establish the rail model consistent with the experimental system for theoretical research. In the FE simulation solution, the grid size in the FE model is 1.5 mm, as shown in figure 3*B*.

$$T \leq \frac{x}{\sqrt{V_L + V_H}} \tag{1}$$

FIG. 1 The experimental system for detecting fatigue cracks in rails using ultrasonic guided waves.

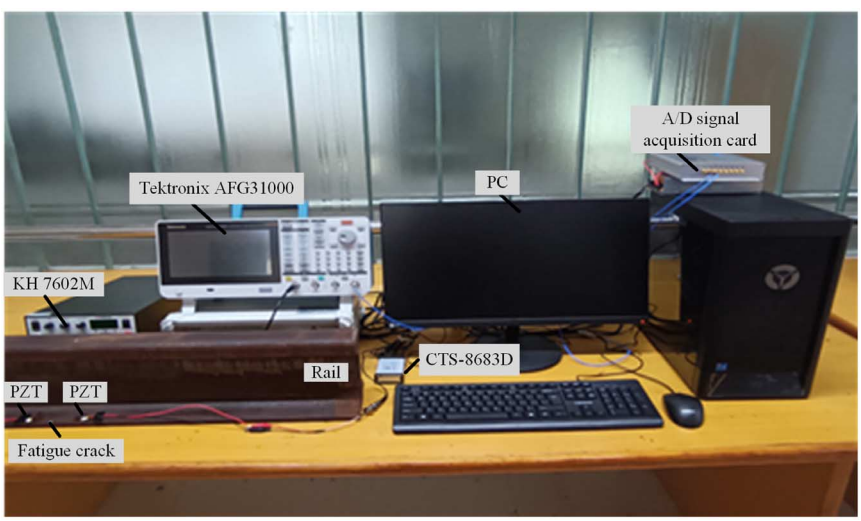

FIG. 2 (*A*) The excitation waveform of ultrasonic guided wave in rail bottom and (*B*) the frequency spectrum of ultrasonic guided waves in rail.

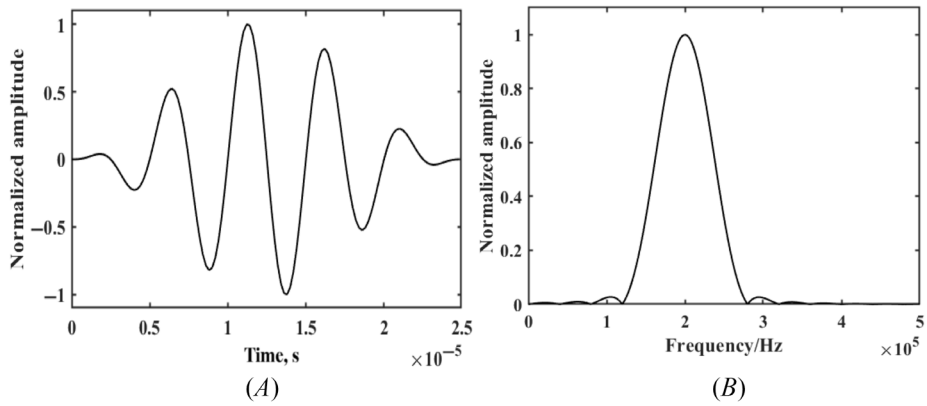

FIG. 3 (*A*) The 3D rail model built by Pro/E software and (*B*) the grid division diagram of FE simulation in the rail.

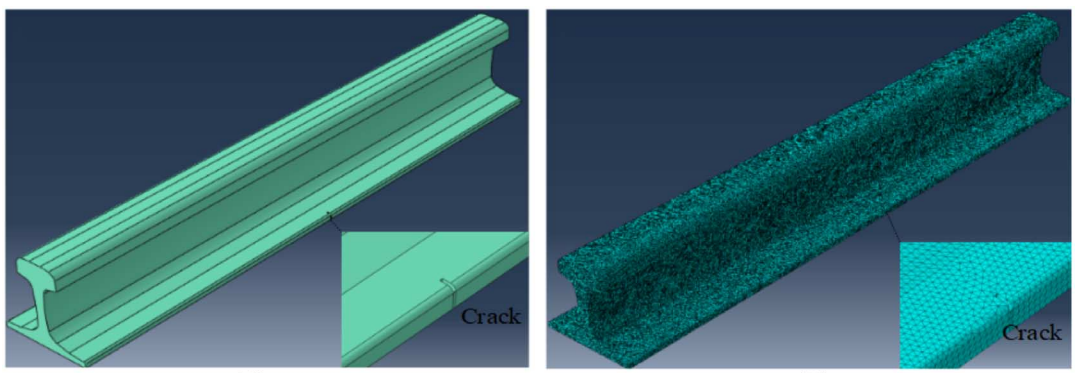

TABLE 1
Material parameters of the rail

Young's Modulus, GPa	Poisson's Ratio	Density, kg/m^3
206	0.3	7,850

The velocities of P-wave (V_L) and S-wave (V_H) in rail are 5,778 m/s and 3,142 m/s respectively, and x represents the grid size in the FE model. The time step (T) needs to be kept less than what is calculated by formula (1). The time step calculated by the formula is 0.228 μs, and the time step of 0.2 μs is selected for the FE model. The total time of the FE model is 200 μs, and the total number of sampling points is 1,001.

PCA

PCA is an unsupervised statistical method of data dimensionality reduction. It mainly maps high-dimensional data to low-dimensional data space through orthogonal transformation and obtains the maximum covariance of sample data. Deng et al. used segmental PCA to extract the features of the ultrasonic wave received at different positions of the rail to realize the classification and identification of different types of railhead defects.[25]

Because there are 6 groups of experimental data and 21 groups of simulation data, the amount of data is less, In order to increase the data sample of the ultrasonic wave, the method of adding random Gaussian white noise in the simulation data set was used. Nine different degrees of random Gaussian white noise (2 dB, 4 dB, 6 dB, 8 dB, 10 dB … 18 dB of the original data) will be added to the simulation data concentration. The ultrasound wave is finally composed of 216 groups, including 210 groups of FE simulation data and 6 groups of experimental data. Then, the characteristics of the different fatigue crack depths of the rail bottom are characterized by PCA, and the five main features are selected for analysis. The five features can characterize the ultrasonic wave, and the cumulative contribution rate of the five features has reached more than 98 %, as shown in figure 4. The scatter diagram of the five main features' distribution is shown in figure 5. It is difficult to effectively identify the fatigue crack depth from the feature data set of the five main components.

The specific steps of extracting the features are as follows. the eigenvector matrix of the ultrasonic guided wave is $X = \{X_1, X_2 \ldots, X_n\}$

FIG. 4

The distribution of the contribution rate of the five main features.

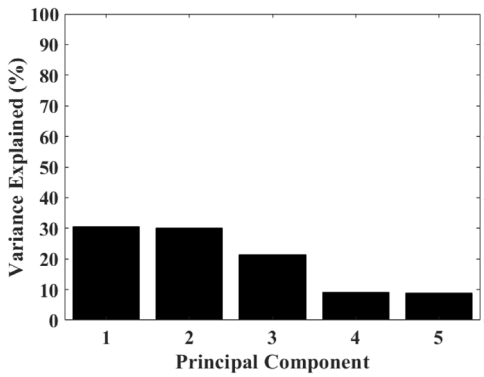

FIG. 5

The scatter diagrams of the five main features' distributions.

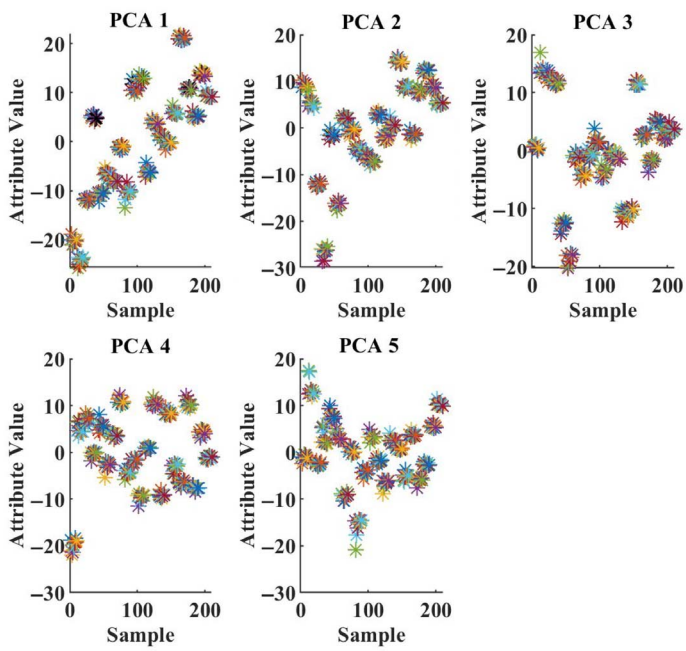

1. Centralize the samples of the ultrasonic guided wave:

$$X_i = X_i - \frac{1}{N}\sum_{i}^{N} X_i \tag{2}$$

2. Calculate the samples' covariance matrix of the ultrasonic guided wave:

$$\mathrm{cov}(X, X^T) = \frac{\sum_{i=1}^{N}(X - \overline{X})(X_i^T - \overline{X^T})}{m-1} \tag{3}$$

3. Calculate the characteristic decomposition of the covariance matrix:

$$\mathrm{cov}(X, X^T)W = \lambda W \tag{4}$$

4. According to the order of eigenvalues, the eigenvalue matrix of the ultrasonic guided wave is obtained, and the five main features are selected for FE model analysis.

In the process of the rail experiment and FE simulation, the flowchart of the PCA-SVM model based on the ultrasonic wave to quantitatively detect the fatigue crack is shown in **figure 6**. Among them, there are 216 experimental and simulation samples in total (80 % of the data is used as an SVM training set, and 20 % of the data is used as an SVM test set). The classification performance of nonlinear SVM is compared with different kernel functions (SVM poly, SVM linear, SVM radial basis function [RBF], and SVM sigmoid).

SVM REGRESSION ALGORITHM

Boser, Guyon, and Vapnik used SVM to carry out regression prediction on the data by introducing ε.[26] The SVM for regression (SVR) is obtained by the insensitive loss function, which has achieved good performance in

FIG. 6 The flowchart of the PCA-SVM model based on the ultrasonic wave to quantitatively detect the rail bottom defects: (*A*) FE simulation, (*B*) feature extraction, and (*C*) GS-SVM model evaluation.

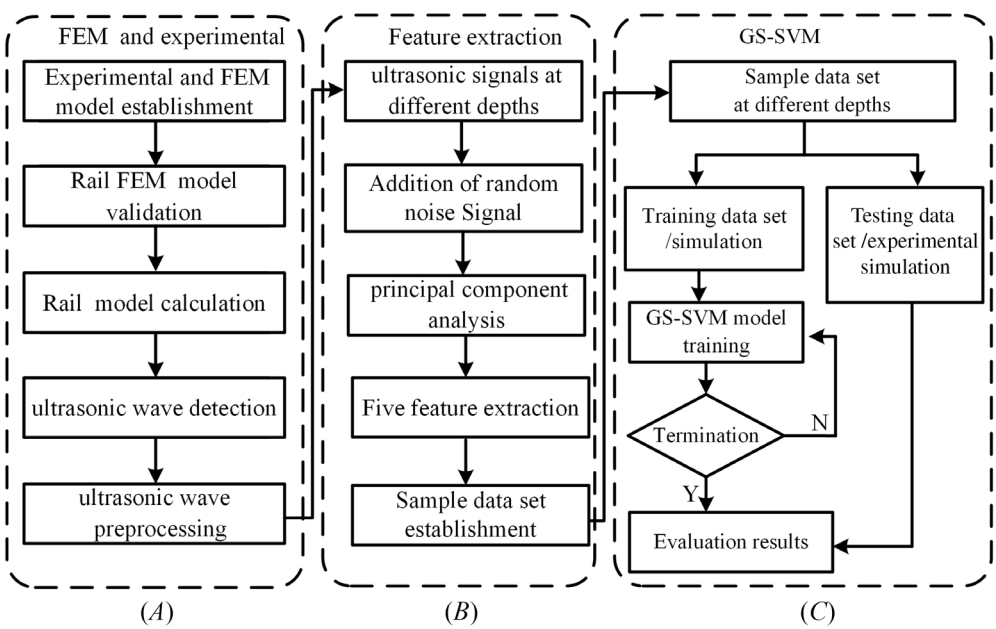

prediction.[27,28] It is proposed to find an optimal classification surface to minimize the error of all training samples from the optimal classification surface. The regression function of SVM is as follows:

$$f(x) = \omega^* \Phi(x) + b^* = \sum_{i=1}^{l} (a_i - a_i^*) \Phi(x_i) \Phi(x) + b^* \tag{5}$$

From equation (5), it can be seen that the final function form of SVR is the same as that of SVM, and its structure is similar to that of the neural network. The output is a linear combination of intermediate nodes, and each intermediate node corresponds to a support vector. The function svmpredict can be used to realize the simulation test of the SVR regression model. The calculation formulas of mean squared error (MSE) and the determination coefficient R^2 are as follows:

$$E = \frac{1}{l} \sum_{i=1}^{l} (\hat{y}_i - y_i)^2 \tag{6}$$

$$R^2 = \frac{(l \sum_{i=1}^{t} (\hat{y}_i y_i - \sum_{i=1}^{t} \hat{y}_i \sum_{i=1}^{t} \hat{y}_i)^2}{(l \sum_{i=1}^{t} \hat{y}_i^2 - (\sum_{i=1}^{t} \hat{y}_i)^2)(l \sum_{i=1}^{t} y_i^2 - (\sum_{i=1}^{t} y_i)^2)} \tag{7}$$

where l is the number of samples in the test set; $y_i (i = 1, 2, \ldots, l)$ is the true value of the ith sample; and $\hat{y}_i (i = 1, 2, \ldots, l)$ is the predicted value of the ith sample. It mainly uses the GS method to find the best parameters: c (penalty factor) and g. The basic idea of GS method is to search for the best combination of the penalty factor c and kernel function parameter g in the whole grid to optimize the performance of SVM and to find out the MSE of SVM at the same time. K-fold cross-validation is used to select the optimal kernel parameters and optimal penalty coefficients of SVM to avoid over fitting. The search method steps are as follows:

1. The selection range of the penalty factor c and the kernel function parameter g is determined:
2. Divide the data set into k training sets and one test set.
3. Get each subset as the test set, repeat the steps in step 2, get each subset as the error prediction of the test set, and select the minimum MSE as the prediction error.
4. Adjust parameters g and c, repeat steps 2 and 3, and select the MSE as the optimal parameter combination for GS. The specific process is shown in **figure 7**

Results and Discussion

The normalized ultrasonic guided wave diagram and the spectrum diagram (the FE simulation results and the experimental results) are obtained when the ultrasonic guided wave passes through the rail with or without the rail fatigue crack, as shown in **figure 8**. As can be seen from **figure 8*A*** and **8*B***, when there is rail fatigue crack at the rail bottom, the simulation waveform results are basically consistent with the experimental waveform results, which shows that the established rail ultrasonic guided wave model is consistent with the actual experimental model. When the rail fatigue crack depth is 2 mm, the ultrasonic guided wave obtained by the FE simulation model is consistent with the ultrasonic guided wave obtained by the experiment, and the amplitude of the ultrasonic guided wave received with the fatigue crack is smaller than that without the rail fatigue crack. This is mainly because some of the ultrasonic waves are reflected by the rail fatigue crack, and the remaining ultrasonic waves are transmitted through the rail crack.

The spectrum of the ultrasonic guided wave with the fatigue crack is narrower than that without the fatigue crack, which indicates that the rail fatigue crack has the characteristic of frequency selection for the ultrasonic wave. The spectrum diagram of the FE simulation results is consistent with the spectrum diagram of the actual

FIG. 7

The flowchart of the SVM model based on the GS method.

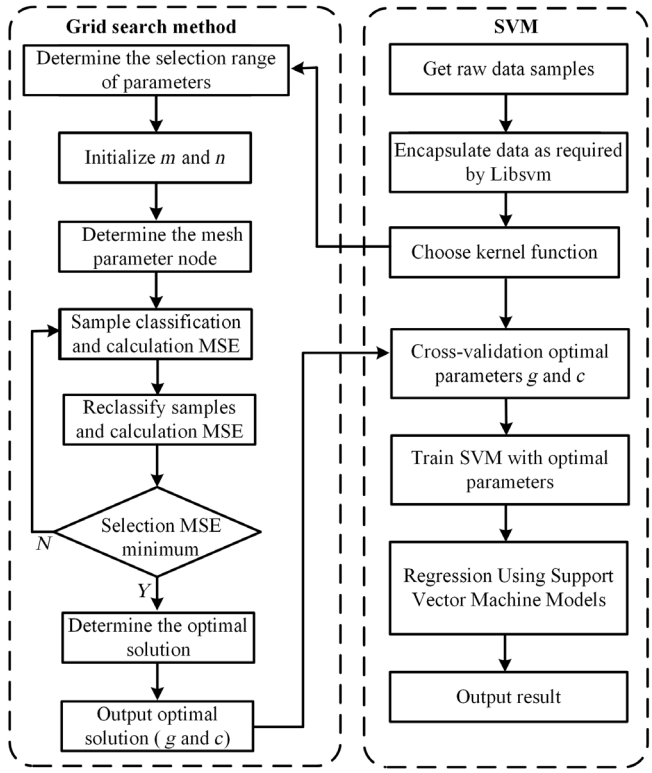

FIG. 8 FE simulation results and experimental results: (*A*) the time domain waveform without the fatigue crack and (*B*) the time domain waveform when the depth of the fatigue crack is 2 mm.

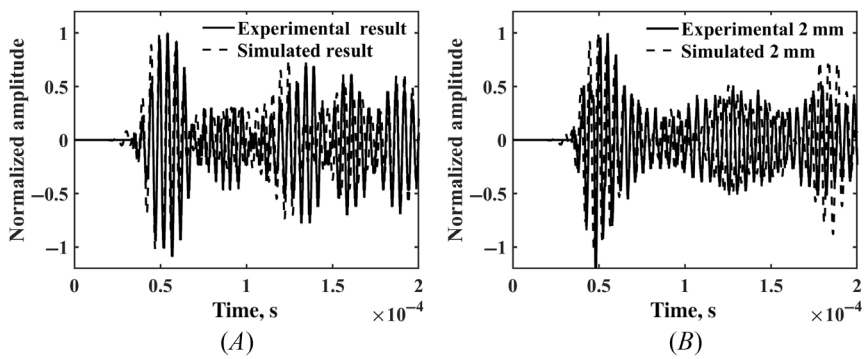

experiments, as can be seen from figure 9*A*–*D*. According to the outlined analysis, the FE simulation model established in this paper can simulate the actual ultrasonic wave to detect the rail fatigue crack.

According to the relevant theory of SVM, the selection of the penalty parameter c and the kernel function parameter g affects the prediction effect of SVM. Therefore, this paper uses the GS method to select the penalty parameter c and the kernel function parameter g. The penalty parameter c and the kernel function parameter g are roughly selected. The selected c is 0.57435, g is 16, and the MSE is 0.028097, as can be seen from figure 10*A* and 10*B*.

FIG. 9 The FE simulation results and experimental results: (*A*) the fast fourier transformation (FFT) without the fatigue crack, (*B*) the FFT when the depth of the fatigue crack is 2 mm, (*C*) the FFT when the depth of the fatigue crack is 4 mm, and (*D*) the FFT when the depth of the fatigue crack is 6 mm.

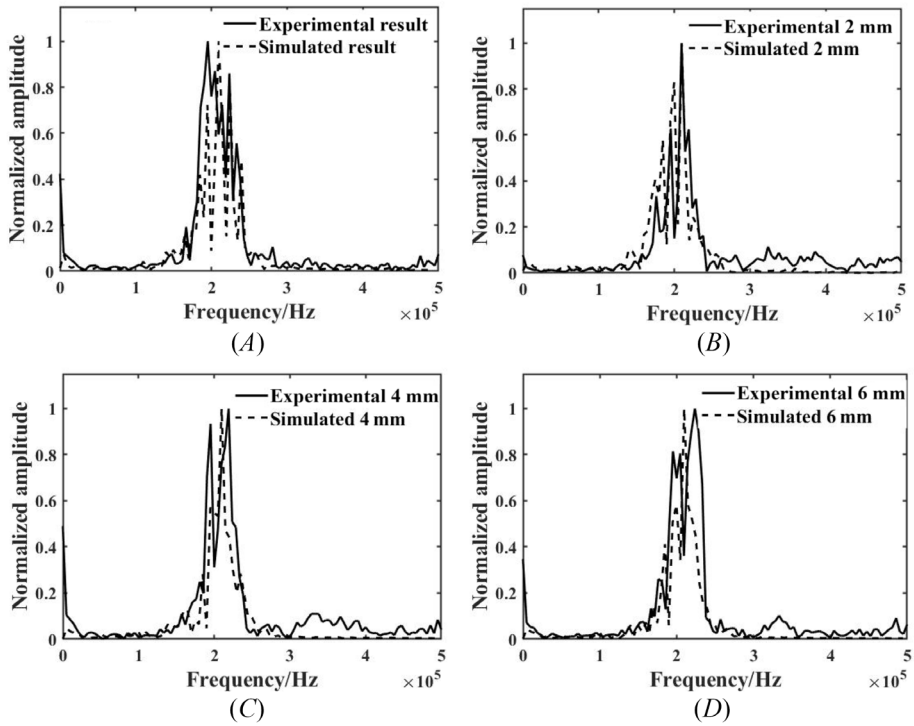

FIG. 10 Rough tuning and optimization of *g* and *c* parameters of SVM: (*A*) the 3D view of mesh parameter optimization and (*B*) the contour map for optimization of grid parameters.

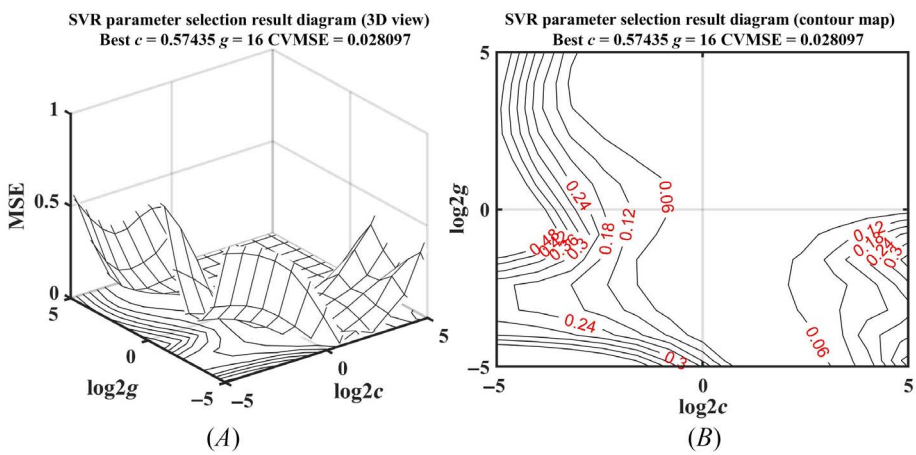

When the best combination area of the *c* and *g* parameters is determined, the *c* and *g* parameters are then carefully selected. The selected *c* is 2.8284, *g* is 5.6569, and the MSE is 0.026367, as shown in figure 11*A* and 11*B*. After two rounds of screening, the optimal penalty parameter *c* and the kernel function parameter *g* are basically determined. At this time, the MSE of SVM is the smallest.

FIG. 11 Fine-tuning and optimization of *g* and *c* parameters of SVM: (*A*) the 3D view of mesh parameter optimization and (*B*) the contour map for optimization of grid parameters.

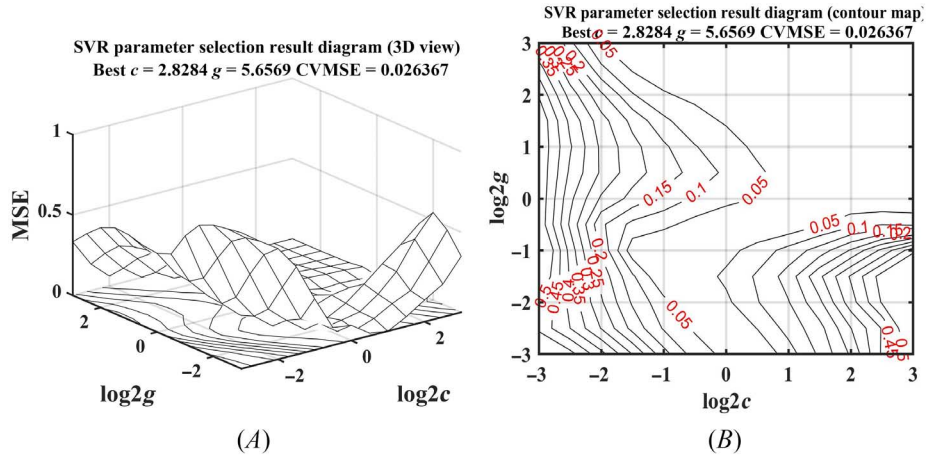

(*A*) (*B*)

According to the GS cross-validation method, the optimal combination of the penalty parameter *c* and the kernel function parameter *g* is obtained. GS-SVM is used to predict the training set and test set prediction results, as shown in **figure 12**. The MSE and determination coefficient R^2 of the training set are 0.00075896 and 0.9979, respectively, as can be seen from **figure 12*A***. The MSE and determination coefficient R^2 of the test set are 0.0011976 and 0.99739 respectively, which shows that the GS-SVM algorithm can accurately predict 43 test sets (including 6 experimental data sets), as shown in **figure 12*B***. In conclusion, the GS-SVM algorithm can predict the fatigue crack depth of the rail bottom and has good performance characteristics.

The results of the predicted value and the actual value obtained by the GS-SVM algorithm are shown in **figure 13*A***. The prediction results of the fatigue crack depth of the rail bottom are in good agreement with the best-fitting straight line, indicating that the fatigue crack depth of the rail bottom predicted by the GS-SVM algorithm is basically consistent with the actual size of the rail fatigue crack, as shown in **figure 13*A***. **Figure 13*B*** shows the relative error between the predicted value and the actual value obtained by the GS-SVM algorithm. It can be seen from **figure 13*B*** that the relative error between the fatigue crack depth

FIG. 12 The fatigue crack depth prediction and the actual results based on SVM: (*A*) the training set (80 %) and (*B*) the test set (20 %).

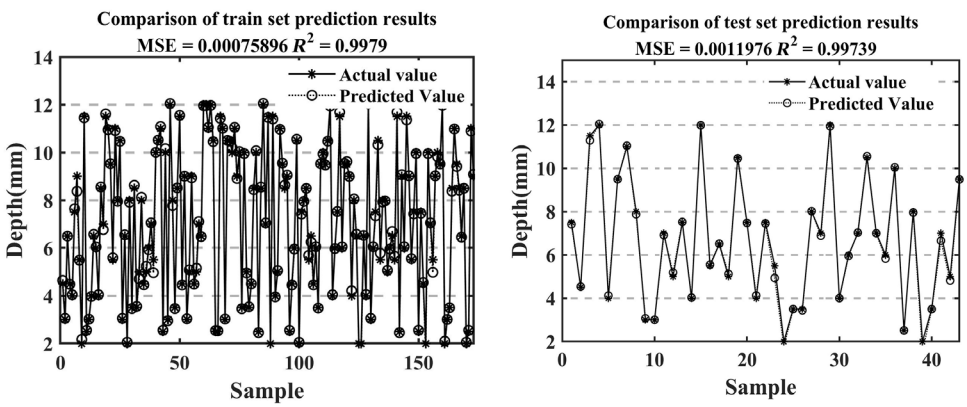

(*A*) (*B*)

FIG. 13 (*A*) Comparison between the predicted value and the actual value based on SVM and (*B*) absolute error between the predicted value and the actual value.

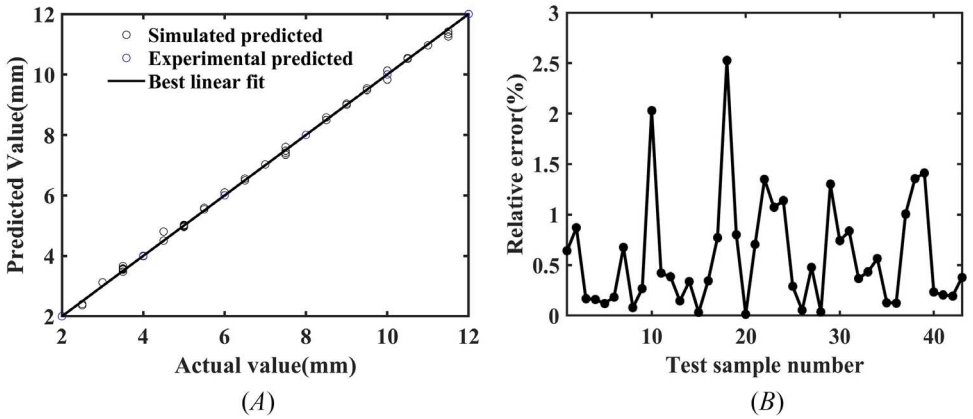

of the rail bottom predicted value and the actual value obtained by the GS-SVM algorithm is within 3.0 %, the maximum relative error is 2.6 %, and the average error is within 1.5 %. The results show that the GS-SVM algorithm is feasible for quantitatively evaluating the fatigue crack depth of the rail bottom. Based on the described analysis, the GS-SVM algorithm proposed in this study has good performance in the quantitative evaluation of the fatigue crack depth of the rail bottom. In this study, the combination of the ultrasonic guided wave technology, FE simulation, PCA, and GS-SVM algorithm is an effective method for quantitatively evaluating the fatigue crack depth of the rail bottom.

The performance comparison of the ultrasonic guided wave based on the GS-SVM algorithm for the rail fatigue depth prediction under different kernel functions is shown in Table 2. It can be seen from the Table 2 that

TABLE 2
Performance comparison of four kernel functions' optimized grid search algorithms

	Linear	Poly	RBF	Sigmoid
Training accuracy, %	99.9848	87.9196	99.79	96.6208
Prediction accuracy, %	87.7283	90.7625	99.739	95.9304
MSE	0.08613	0.067	0.026367	0.03619
c	1	5.6287	2.8284	2.9532
g	16	3.5687	5.6569	1
Running time, s	5.106740	25.34613	2.066	1.96136

FIG. 14
The evaluation of GS-SVM with four kernel functions.

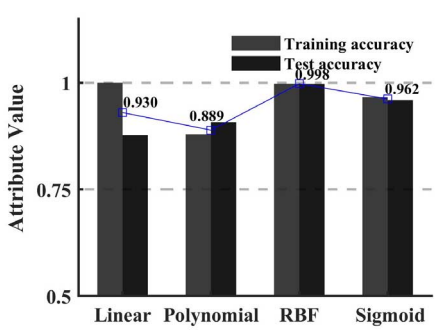

when the kernel functions are linear, poly, RBF, and sigmoid, the accuracy of the prediction model in the training set is 99.9848 %, 87.9196 %, 99.79 %, and 99.6208 %, respectively, and the accuracy of the prediction model in the test set is 87.7283 %, 90.7625 %, 99.739 %, and 95.9304 %, respectively. The program running time of the prediction model is 5.106740 s, 25.34613 s, 2.066 s, and 1.96136 s, respectively, and the MSE of the prediction model is 0.08613, 0.067, 0.026367, and 0.03619, respectively. Among the four kernel functions, the RBF kernel function has the best comprehensive performance, as shown in **figure 14**.

Conclusion

In this paper, an ultrasonic guided wave method based on the GS-SVM model is proposed to predict and quantitatively evaluate the different depths of the rail bottom fatigue cracks. Firstly, the FE model of the ultrasonic guided wave in the rail bottom fatigue cracks are established, and the ultrasonic guided wave detection system is built. The ultrasonic guided wave (the FE simulation and the experimental data set) under the different depths of the rail bottom fatigue cracks are obtained. The PCA method is then used to extract the five main important features of the ultrasonic guided waves for the GS-SVM model training and prediction. The results show that the GS-SVM model proposed in this study has good performance in the quantitative evaluation of different depths of rail bottom fatigue cracks, and the method of quantitative evaluation of different depths of rail bottom fatigue cracks by the GS-SVM model is feasible.

In this study, the FE model was used to generate the data for model training and validation. Although it has been validated by experimental results, we could not guarantee that statistic features of FE data are the same as that of experimental results for all the crack depth scenarios. Therefore, we will use transfer learning to resolve the domain adaptation problem in the future work.

ACKNOWLEDGMENTS

This work was supported by the National Natural Science Foundation of China (62061021). Jiangxi Provincial Natural Science Foundation (20202BABL201024), Jiujiang Double Hundred and Double Thousand Talent Project, and Jiangxi Provincial Department of Education Science and Technology Project (GJJ170959).

References

1. X. Xining, Z. Lu, X. Bo, Y. Zujun, and Z. Liqiang, "An Ultrasonic Guided Wave Mode Excitation Method in Rails," *IEEE Access* 6 (October 2018): 60414–60428, http://dx.doi.org/10.1109/ACCESS.2018.2875123
2. M. Masmoudi, S. Yaacoubi, M. Koabaz, M. Akrout, and A. Skaiky, "On the Use of Ultrasonic Guided Waves for the Health Monitoring of Rails," *Proceedings of the Institution of Mechanical Engineers, Part F: Journal of Rail* 236, no. 5 (May 2022): 469–489, http://dx.doi.org/10.1177/09544097211025898
3. J. Wu, Z. Tang, F. Lü, and K. Yang, "Ultrasonic Guided Wave Focusing in Waveguides with Constant Irregular Cross-Sections," *Ultrasonics* 89 (September 2018): 1–12, https://doi.org/10.1016/j.ultras.2018.04.003
4. J. Xie, W. Ding, W. Zou, T. Wang, and J. Yang, "Defect Detection inside a Rail Head by Ultrasonic Guided Waves," *Symmetry* 14, no. 12 (December 2022): 2566, https://doi.org/10.3390/sym14122566
5. P. W. Loveday, C. S. Long, and D. A. Ramatlo, "Mode Repulsion of Ultrasonic Guided Waves in Rails," *Ultrasonics* 84, no. 5 (March 2018): 341–349, https://dx.doi.org/10.1016/j.ultras.2017.11.014
6. Z. Tang, W. Liu, R. Yan, P. Zhang, F. Lv, and X. Chen, "Application of Compressed Sensing in the Guided Wave Structural Health Monitoring of Switch Rails," *Measurement Science and Technology* 32, no. 12 (September 2021): 125112, https://doi.org/10.1088/1361-6501/ac2316
7. S. Coccia, R. Phillips, C. Nucera, I. Bartoli, S. Salamone, F. L. di Scalea, M. Fateh, and G. Carr, "Non-contact Ultrasonic Guided-Wave Defect Detection System for Rails: An Update," *Sensors and Smart Structures Technologies for Civil, Mechanical, and Aerospace Systems 2011 Proceedings* 7981 (April 2011): 798113, https://dx.doi.org/10.1117/12.880238
8. S. Mariani, T. V. Nguyen, X. Zhu, S. Sternini, F. L. di Scalea, M. Fateh, and R. Wilson, "Non-contact Ultrasonic Guided Wave Inspection of Rails: Next Generation Approach," *Proceedings of the 2016 Joint Rail Conference: 2016 Joint Rail Conference* (New York: American Society of Mechanical Engineers, 2016), V001T06A011, http://dx.doi.org/10.1115/JRC2016-5771
9. D. A. Ramatlo, C. S. Long, P. W. Loveday, and D. N. Wilke, "A Modelling Framework for Simulation of Ultrasonic Guided Wave-Based Inspection of Welded Rail Tracks," *Ultrasonics* 108 (2020): 106215–106215, https://doi.org/10.1016/j.ultras.2020.106215

10. M. H. S. Siqueira, C. E. N. Gatts, R. R. da Silva, and J. M. A. Rebello, "The Use of Ultrasonic Guided Waves and Wavelets Analysis in Pipe Inspection," *Ultrasonics* 41, no. 10 (May 2004): 785–797, https://doi.org/10.1016/j.ultras.2004.02.013
11. T. Hayashi, W.-J. Song, and J. L. Rose, "Guided Wave Dispersion Curves for a Bar with an Arbitrary Cross-Section, a Rod and Rail Example," *Ultrasonics* 41, no. 3 (May 2003): 175–183, https://doi.org/10.1016/S0041-624X(03)00097-0
12. I. Bartoli, F. L. di Scalea, M. Fateh, and E. Viola, "Modeling Guided Wave Propagation with Application to the Long-Range Defect Detection in Railroad Tracks," *NDT & E International* 38, no. 5 (July 2005): 325–334, https://doi.org/10.1016/j.ndteint.2004.10.008
13. H. Taweel, S. B. Dong, and M. Kazic, "Wave Reflection from the Free End of a Cylinder with an Arbitrary Cross-Section," *International Journal of Solids and Structures* 37, no. 12 (March 2000): 1701–1726, https://doi.org/10.1016/S0020-7683(98)00301-1
14. S. Coccia, I. Bartoli, A. Marzani, F. Lanza di Scalea, S. Salamone, and M. Fateh, "Numerical and Experimental Study of Guided Waves for Detection of Defects in the Rail Head," *NDT & E International* 44, no. 1 (January 2011): 93–100, https://doi.org/10.1016/j.ndteint.2010.09.011
15. T. Hayashi, Y. Miyazaki, M. Murase, and T. Abe, "Guided Wave Inspection for Bottom Edge of Rails," *AIP Conference Proceedings* 894, no. 1 (March 2007): 169–176, https://doi.org/10.1063/1.2717970
16. R. M. Sanderson and S. D. Smith, "The Application of Finite Element Modelling to Guided Wave Testing Systems," *AIP Conference Proceedings* 657, no. 1 (April 2003): 256–263, https://doi.org/10.1063/1.1570145
17. S. B. Palmer, S. Dixon, R. S. Edwards, and X. Jian, "Transverse and Longitudinal Crack Detection in the Head of Rail Tracks Using Rayleigh Wave-Like Wideband Guided Ultrasonic Waves," *Nondestructive Evaluation and Health Monitoring of Aerospace Materials, Composites, and Civil Infrastructure IV* 5767 (May 2005): 70–80, https://doi.org/10.1117/12.598142
18. S. Moustakidis, V. Kappatos, P. Karlsson, C. Selcuk, T.-H. Gan, and K. Hrissagis, "An Intelligent Methodology for Railways Monitoring Using Ultrasonic Guided Waves," *Journal of Nondestructive Evaluation* 33, no. 4 (October 2014): 694–710, https://doi.org/10.1007/s10921-014-0264-6
19. H. Cunfu, Q. Liu, J. Jiao, F. Liu, and B. Wu, "Numerical Calculation of Propagation Characteristics of Ultrasonic Guided Waves in Rails Based on Vibration Modal Analysis Method" (in Chinese), *Journal of Vibration and Shock* 33, no. 3 (2014): 9–13, https://doi.org/10.13465/j.cnki.jvs.2014.03.003
20. P. Hu, H. Wang, G. Tian, Z. Dong, F. Qiu, and B. F. Spencer, "Wireless Localization of Spallings in Switch-Rails with Guided Waves Based on a Time–Frequency Method," *IEEE Sensors Journal* 19, no. 23 (August 2019): 11050–11062, https://doi.org/10.1109/JSEN.2019.2934159
21. P. Hu, H. T. Wang, G. Y. Tian, Y. Liu, X. Li, and B. F. Spencer, "Multifunctional Flexible Sensor Array-Based Damage Monitoring for Switch Rail Using Passive and Active Sensing," *Smart Materials and Structures* 29, no. 9 (August 2020): 095013, https://doi.org/10.1088/1361-665X/ab9e0f
22. H. Mahajan and S. Banerjee, "A Machine Learning Framework for Guided Wave-Based Damage Detection of Rail Head Using Surface-Bonded Piezo-Electric Wafer Transducers," *Machine Learning with Applications* 7 (March 2022): 100216, https://doi.org/10.1016/j.mlwa.2021.100216
23. Y. Yu, W. Li, J. Li, and T. N. Nguyen, "A Novel Optimised Self-Learning Method for Compressive Strength Prediction of High Performance Concrete," *Construction and Building Materials* 184, no. 9 (September 2018): 229–247, https://doi.org/10.1016/j.conbuildmat.2018.06.219
24. Y. Yu, Y. Li, J. Li, and X. Gu, "Self-Adaptive Step Fruit Fly Algorithm Optimized Support Vector Regression Model for Dynamic Response Prediction of Magnetorheological Elastomer Base Isolator," *Neurocomputing* 211 (October 2016): 41–52, http://dx.doi.org/10.1016/j.neucom.2016.02.074
25. F. Deng, S.-Q. Li, X.-R. Zhang, L. Zhao, J.-B. Huang, and C. Zhou, "An Intelligence Method for Recognizing Multiple Defects in Rail," *Sensors* 21, no. 23 (December 2021): 8108, https://doi.org/10.3390/s21238108
26. B. E. Boser, I. M. Guyon, and V. N. Vapnik, "A Training Algorithm for Optimal Margin Classifiers," in *COLT '92: Proceedings of the Fifth Annual Workshop on Computational Learning Theory* (New York: Association for Computing Machinery, 1992), 144–152, https://dx.doi.org/10.1145/130385.130401
27. Y. Yu, Y. Li, and J. Li, "Forecasting Hysteresis Behaviours of Magnetorheological Elastomer Base Isolator Utilizing a Hybrid Model Based on Support Vector Regression and Improved Particle Swarm Optimization," *Smart Materials and Structures* 24, no. 3 (February 2015): 035025, https://doi.org/10.1088/0964-1726/24/3/035025
28. Y. Yu, C. Zhang, X. Gu, and Y. Cui, "Expansion Prediction of Alkali Aggregate Reactivity-Affected Concrete Structures Using a Hybrid Soft Computing Method," *Neural Computing and Applications* 31, no. 12 (December 2019): 8641–8660, https://doi.org/10.1007/s00521-018-3679-7